RSC Advances

ROYAL SOCIETY OF CHEMISTRY

www.rsc.org/advances

Journal Name

ARTICLE

Biocompatible succinic acid-based polyesters for potential biomedical applications: fungal biofilm inhibition and mesenchymal stem cells growth

Received 00th January 20xx,
Accepted 00th January 20xx

DOI: 10.1039/x0xx00000x

www.rsc.org/

E. Jäger,[a,b*] R.K. Donato,[c,*] M. Perchacz,[a,b] A. Jäger,[a,b] F. Surman,[a] A. Höcherl,[a] R. Konefał,[a,b] K.Z. Donato,[c] C.G. Venturini,[a] V.Z. Bergamo,[d] H.S. Schrekker,[c] A.M. Fuentefria,[d] M.G. Raucci,[e] L. Ambrosio[e] and P. Štěpánek[a]

Herein, we present the intrinsic property of well-known polyesters [poly(alkene succinates)], as *Candida albicans* and *Candida tropicalis* biofilm inhibitors with potential to substantially reduce the incidence of device-associated infections in, *e.g.*, indwelling catheters and sutures. These new biopolymer applications either for manufacturing or coating medical devices, present innovative features such as; simple and cheap preparation, easy scaling-up, good mechanical and thermal resistance properties, and antibiofilm ability without any specific surface functionalization or antimicrobial agents encapsulation. Furthermore, the polyesters are shown to be highly biocompatible, promote human mesenchymal stem cells (hMSC) attachment and proliferation, inducing morphological changes, which are dependent on the polymer structural characteristics, making them promising candidates for materials in specialized medical devices and in the tissue engineering field.

Introduction

In most of the fields of medicine, the implantation or insertion of foreign bodies has become a routine and indispensable procedure. In this context, the use of biodegradable/biocompatible polymers for invasive medical devices and implants presents a broad range of advantages over conventional materials. Among the most important are the avoidance of a second surgical process for their removal and the gradual transition between the function applied by the material and the organism recovery, avoiding inflammatory processes.[1] As a consequence of the recent developments in this area, several biomedical sectors have reported a huge increase in biopolymer application, where the production of biodegradable/biocompatible sutures alone represents a market exceeding $1.3 billion annually.[2]

Nowadays, most of the medical devices are associated with a constant microbial infection risk, which significantly contributes to the increasing nosocomial infections problem.[3] There has been a substantial increase in device-related infections which is attributed to biofilm forming fungi, such as *Candida* spp. The biofilm formation facilitates their adhesion to devices and renders them relatively refractory to medical therapy. Generally, removal of the infected device is inevitable to establish a cure of *Candida* infections.[4]

Candida albicans are opportunistic fungi that cause several systemic fungal infections in humans,[5,6] and have emerged as important morbidity and mortality causes in immunocompromised patients, *e.g.*, AIDS, cancer chemotherapy, organ or bone marrow transplanted patients.[7-9] In addition, hospital-acquired infections by *C. albicans* have become a major health concern due to fungal colonization in the human body on implanted medical devices where biofilms can develop within hours.[10,11] *Candida* biofilm cells are many times (30-2000 times) more resistant than planktonic cells against diverse antifungal agents, including amphotericin B (AmB) and azolics like fluconazole.[12,13] Although *C. albicans* biofilms formation is the most responsible etiologic agent in candidiasis infections, *C. tropicalis* is an important pathogenic biofilm producer among the non-albicans *Candida* species[14,15] which is currently considered as an emerging multidrug-resistent pathogen of medical importance. Altogether, catheter-related bloodstream infections by *Candida* spp. have increased

[a] Institute of Macromolecular Chemistry v.v.i., Academy of Sciences of the Czech Republic, Heyrovsky Sq. 2, 162 06 Prague 6, Czech Republic.
[b] Charles University Prague, Faculty of Natural Sciences, Hlavova 2030, Prague 12840 2, Czech Republic.
[c] Laboratory of Technological Processes and Catalysis, Institute of Chemistry, Universidade Federal do Rio Grande do Sul. Av. Bento Gonçalves 9500, Porto Alegre, RS, CEP: 91.501-970, Brazil.
[d] Laboratory of Applied Mycology, Department of Analysis, Faculty of Pharmacy, Universidade Federal do Rio Grande do Sul, Av. Ipiranga 2752, Porto Alegre, RS, CEP: 90.610-000, Brazil.
[e] Institute of Polymers, Composites and Biomaterials, National Research Council of Italy, Mostrad'Oltremare Pad.20, Viale Kennedy 54, Naples, Italy.
E-mail: jager@imc.cas.cz; donatork@gmail.com; Tel: +420 296 809 296.
† Footnotes relating to the title and/or authors should appear here.
Electronic Supplementary Information (ESI) available: [details of any supplementary information available should be included here]. See DOI: 10.1039/x0xx00000x

intensely in the last years,[16] mainly commiting critically ill patients on a global scale.[17,18]

These device biofilm infections come together with another serious consequence as the host defense mechanisms are often unable to eliminate the microorganisms from the colonized foreign bodies and the device itself becomes a subject of rejection.[3] Thus, designing biomaterials which intrinsically prevent biofilm-associated infections, while avoiding the toxicity to the human host, is a challenging endeavor.[19-21] Therefore, the use of common human metabolites as monomers for biopolymer synthesis offers a route that minimizes toxic side effects, as during degradation they release molecules that the body can resorb, metabolizing them in various physiological pathways.[22] In addition, especially in the case of sutures and implants, the use of biopolymers which can help tissue regeneration becomes also attractive[23] because as opposed to conventional materials, biopolymers can significantly influence the growth and morphology of mesenchymal stem cells (MSCs). Studies have shown that differentiation of MSCs along the osteogenic pathway appears to be highly dependent on the substrate (biopolymer) composition,[24] making the applications of biopolymers on MSCs growth and differentiation an open field of exploration. It is important to highlight that regenerative medicine is a potential exciting aspect of the novel therapeutic methods nowadays under development. However, these cultures are easily committed by microorganism contaminations, especially highly proliferative ones, *e.g.*, fungi.[25]

Within this context, herein we present a complete study on the synthesis of a series of succinic acid based polyesters; poly(ethylene succinate) (PES), poly(propylene succinate) (PPS) and poly(butylene succinate) (PBS). The biopolymers' mechanical and thermal properties, biocompatibility, hemolytic activities and anti-biofilm formation properties, as well as their promotion of human mesenchymal stem cells (hMSC) attachment and proliferation were evaluated and compared to those of; (i) polyvinyl chloride (PVC) catheter, (ii) polycaprolactone (PCL) polymer as a model for a biodegradable suture.

Results and Discussion

Structural and thermo-mechanical characterization

The synthetic strategy for polyester synthesis involved two different steps according to the environmentally benign melt polycondensation approach, using commercially available "green" monomers, which have been detailed elsewhere.[26] Samples of similar molecular weight were prepared with the purpose of studying the influence of polyester structure on the final mechanical and thermal properties, surface wettability, biocompatibility, hemolytic activities, anti-biofilm activity and human MSC (hMSC) growth. The polyesters presented white (PES and PBS) to yellowish-brown colours (PPS). Their stiffness varied according to the chemical structure, where PES was the stiffest and PPS was the softest, in accordance with previous observations by other authors.[26,27] The physicochemical characteristics of the synthesized PES, PPS and PBS polyesters, as well as the used control polymers, a[re] shown in Table 1.

The number-average molecular weight (M_n) of the prepared polymers was estimated by SEC comprehending valu[es] between ~ 25.1 kDa for PBS polyester to ~ 28.7 kDa for PPS, holding a reasonable degree of polydispersity, where PES polyester presented the highest value (M_w/M_n = 1.66) (Table 1). The compositions of the prepared polyesters (Fig. 1) were determined by ^{1}H NMR and ^{13}C NMR. As seen by ^{1}H NMR, the PES's succinic acid methylene (B) protons appear at δ = 2.55 - 2.67 ppm and ethylene glycol methylene (A) protons appear at δ = 4.18 - 4.3 ppm (Fig. 1.1a). The PES's ^{13}C NMR (Fig. 1.1b) succinic acid methylene group (B) signal is at δ = 29.1 ppm, and carbonyl group (C) is at δ = 175.2 ppm. Ethylene glycol repeating unit carbons appear at 63.2 ppm (A). The PPS's ^{1}H NMR signal, as seen in Fig. 1.2a, of the succinic ac[id] methylene (B) protons appear as a singlet at δ = 2.62 pp[m] while the propylene glycol methylene (A triplet, C pentet) protons are at δ = 4.16 and 1.96 ppm, respectively. The PPS's ^{13}C NMR (Fig.1.2b) signals of the succinic acid methylene (B) group is at δ = 29.0 ppm and carbonyl (D) group at δ = 172.2 ppm. The propylene glycol carbon unit appears at δ = 61.3 ppm (A) and δ = 27.9 ppm (C). For the PBS's ^{1}H NMR, the tw[o] singlet at δ = 2.63 ppm (A) and δ = 1.60 ppm (B) are attributed to the methylene protons of butanediol, while the other singlet at 1.6 ppm (C) is attributed to the succinic acid protons (Fig. 1.3a). The ^{13}C NMR (Fig. 1.3b) signals of the succinic acid methylene (C) group unit are at δ = 29.1 ppm and carbonyl (D) group unit at δ = 172.2 ppm. Butanediol carbon unit appear at δ = 63.2 ppm (A) and δ = 15.2 ppm (B).

The thermogravimetric analysis (TGA) and the derivative thermal analysis (DTG) of the samples show the initi[al] decomposition temperatures (T_{d10} and T_{d20}), *e.g.*, the temperature at which the polymers show the first signs of decomposition; and the main decomposition temperatures (T_{d50} and T_{dmax}), *e.g.*, the temperatures at which the polymers are suffering severe decomposition (Supplementary information Fig. S1). PPS was the polymer presenting the highest initial thermal decomposition temperatures (T_{d10} and T_{d20}), while PES started decomposing at a 50 °C lower temperature than PPS (Tab. 1). PPS and PBS present a difference between initial decomposition temperatures and the maximum decomposition event in the range of 40 °C, showing a narrow DTG peak, a probable reflex of their smaller polydispersity values (Tab. 1, Fig. S1). PES presents much broader events, suggesting more heterogeneous structure decompositions (Tab. 1).

From the DSC measurements, PCL showed the lowest T_g values of all the polyesters evaluated (Tab. 1). This was expected due to PCL's semi-crystallinity, probably presenting the most crystalline structure among the tested polymers. The synthesized polyesters presented higher T_g values than PC[L] (Tab. 1), however, similar to the values presented in t[he] literature.[21,22] The polyesters' crystallinities were also reported and the PPS had the least crystalline structure, as a probab[le] result of the odd-even effect.[26]

Tab. 1 Physico-chemical and thermal properties of the synthesized polyesters and reference polymers.

Sample	M_n (g.mol^{-1})[a]	M_w (g.mol^{-1})[a]	M_w/M_n (g.mol^{-1})	T_g (° C)[b]	T_{d10} (° C)[c]	T_{d20} (° C)[d]	T_{d50} (° C)[e]	T_{dmax} (° C)[f]
PES	27 510	37 260	1.66	-9	302	323	357	368
PPS	28 710	40 920	1.42	-29	351	366	386	391
PBS	25 060	37 310	1.49	-32	343	361	383	392
PCL	10 000	14 000	1.40	-60	-	-	-	-

[a]Measured by SEC. [b] Measured by DSC. [c] T. for 10 wt.-% loss, determined by TGA; [d] T. for 20 wt.-% loss, determined by TGA; [e] T. for 50 wt.-% loss, determined by TGA; [f] T. of the most intense decomposition peak, determined by DTG.

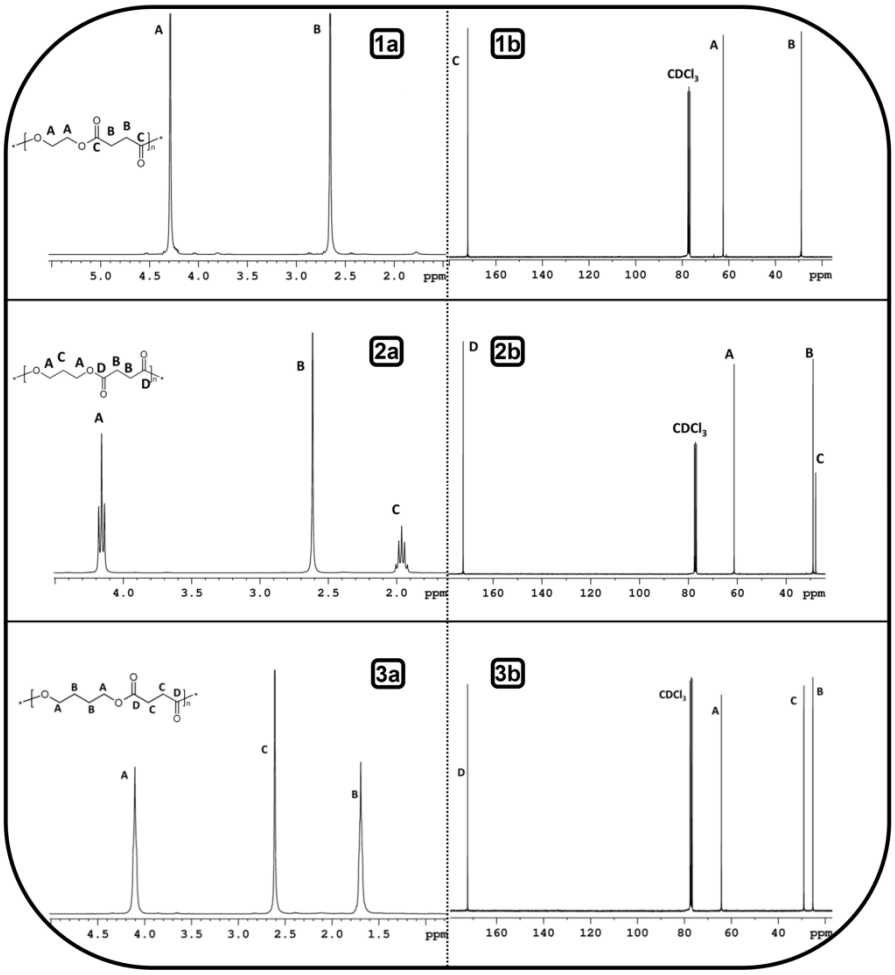

Fig. 1 ^{1}H (a) and ^{13}C (b) NMR of the poly(ethylene succinate) (1), poly(propylene succinate) (2) and poly(butylene succinate) (3) polyesters.

Then, the thermo-mechanical properties of synthesized biopolymers (PES, PPS, PBS) and the commercial catheter (PVC) were followed by dynamic mechanical and thermal analysis (DMTA). Table 2 presents dynamic storage (*G*') and loss (*G*") shear moduli at 25 °C as well as the α-transition temperatures (T_α) of catheter and biopolymers prepared using the melting method.

The prepared polyester materials showed significantly higher shear storage modulus than the model catheter. The long chains of polyesters led to an increase in free volume of the final materials likely causing reduction in the α-transition temperatures. It is visible that the polydispersity of PPS polymer was the lowest due to narrower tan(δ) peak (Loss factor) (Fig. 2.1a, Tab. 1). Moreover, the model catheter showed a complex molecular weight of the polyvinyl chloride used in production (broad tan(δ), Fig. 2.1a).

The relative crystallinity of used polymers was evaluated by comparing the slope of the storage modulus curve (Fig. 2.1 *vs* 2.2). PPS showed to have the largest amorphous segments (Fig. 2.1 *vs*2.2c; Tab. 2), in opposition to PES and PBS, which were much more crystalline (Fig. 2.1 *vs*. 2.2a and b). This also can be seen as as influence to the higher shear storage moduli of PES and PBS polyesters (Tab. 2). Moreover, the low content of small crystals in the PPS caused their early melting around 2 °C.

Tab. 2. Mechanical properties of the different polymers evaluated

Polymer	T_α (°C)	*G*' at 25 °C (MPa)	*G*'' at 25 °C (MPa)	Young modulus (MPa)	Energy to break (mJ/mm^3)	Tensile strength (MPa)	Elongation at break (%)
PVC	17.9	37.5	13.2	14.8	0.51	2.7	30.8
PES	1.2	628	47.1	716.8	1.28	23.8	7.3
PPS	-24.8	91.9	3.2	188.2	0.019	2.2	1.5
PBS	-16.9	187	7.4	704.4	0.83	26.5	5.3

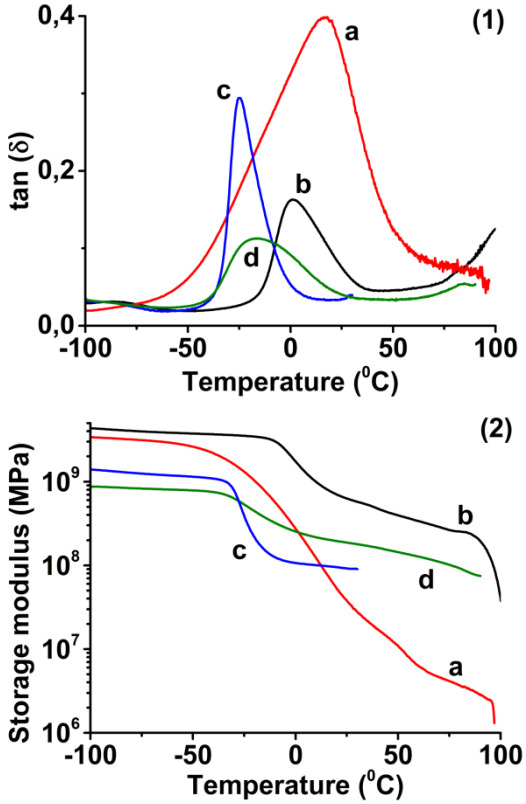

Fig. **2** Loss factor ((tan(δ)) (1) and shear storage modulus (2) as a function of temperature for the: (a) polyvinyl chloride commercial catheter, (b) poly(ethylene succinate), (c) poly(propylene) succinate and (d) poly(butylene) succinate biopolymers, respectively.

The mechanical parameters of the polyester materials and model catheter were depicted in Table 2 and Fig. 3. It can be seen that the most elastic polymer was the PVC catheter due to its high elongation at break (30.8%), but presenting a low Young modulus (14.8 MPa). In contrast, the PES and PBS polyesters showed significantly higher stiffness and toughness, which corresponds to the higher Young modulus, tensile strength and energy to break observed (Tab. 2). The good toughness values suggest the use of PES and PBS for medical devices coating, reinforcing the surface without losing the elongation properties. Accordingly, the worst mechanical properties were observed for the PPS polyester (Tab. 3, Fig. 3) showing general poor mechanical properties. As previously described and in agreement with our experimental data,[26,27] the PPS is the softest biopolymer showing low energy to break, tensile strength and elongation at break (Tab. 3, Fig 3.).

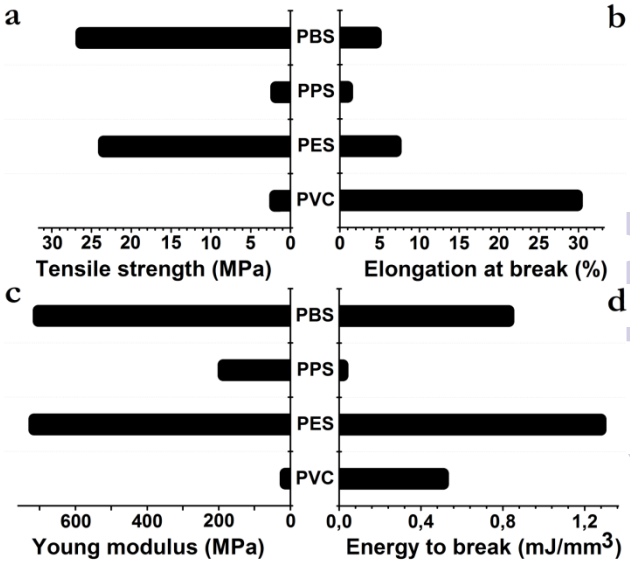

Fig. **3** Tensile strengh (a), elongation at break (b), Young moduli (c) and energy to break (d) of the synthesized biopolymers and PVC.

Antifungal/biofilm properties

All polymers produced in this work were analyzed for their capacity to inhibit the development of *C. tropicalis*, a strong biofilm-producer, which increases the infection treatment difficulty in immunosuppressed patients and represents a source for reinfections in hospitals.[14,28] The inherent antibiofilm ability of materials (especially biocompatible ones) suggests them as potential new prime materials for medical tool set devices, *e.g.* surgical instrumentation and catheters. Thus, the anti-biofilm capacity of each polymer was compared to both a PVC based commercial catheter and PCL. PCL is a polymer that presents antibiofilm properties[29] and serves as a parameter for antimicrobial adhesion.

For isolate 72A (Fluconazole, Amphotericin B (AmB), Voriconazole and Anidulafungin resistant clinical isolate of *C. tropicalis*), all the polymers presented better antibiofilm properties than the commercial catheter. Only PES and PBS presented similar performances to PCL, which completely avoided the formation of biofilm. For isolate 72P (same susceptibility profile), only PBS presented higher biofilm formation than the commercial catheter. The results varied for the different isolates but PPS and PES presented a stronger antibiofilm effect than the PVC commercial catheter for both isolates (Tab. 3).

The polymer that presented the best performance (PES), as well as PCL and PVC commercial catheter (references), were

subsequently submitted for evaluating the effect against *C. albicans* strains (a clinical isolate and a commercial strain of *C. albicans*) biofilm producers. *C. albicans* is the most prevalent pathogenic Candida specie and represents an important public health challenge, especially due to its involvement to the high morbidity and mortality rates of immunocompromised patients.[7,30] It presents strong adherence and biofilm formation on host tissues and medical devices, resulting in increased resistance to antimicrobial agents.[31] Both PCL and PES avoided the biofilm formation from the *C. albicans* strains, but only PES could completely avoid the biofilm formation of all the isolates from both *C. tropicalis* and *C. albicans*, outperforming PCL as an anti-biofilm material (Tab. 3). For this reason the PES polymer might be considered as an antibiofilm polymer with high potential as prime material for medical devices with intrinsic antimicrobial properties.

To obtain an estimation of the polymer surface wettability, contact angle measurements were performed on polymer-coated glass slides. The advancing (θ_{adv}) and receding (θ_{rec}) angles were determined for the synthesized PES, PPS and PBS biopolymers and the results were compared to the PCL polymer, as summarized in Table 3.

Surface wettability is an important feature for evaluating the fungal biofilm adhesion at the polymer surface. This allows us to imply how much of the polymer antibiofilm activity is a reflection of the weak biofilm adhesion at the polymer surface or an effect of the polymer chemical composition on the fungal development. Lower contact angle values indicate more hydrophilic polymer surfaces[32,33] as was observed for the PES biopolymer. As depicted in Tab. 3, all the synthesized polyesters have shown lower values of contact angles in comparison with the PCL polymer. The PES showed the lowest θ_{adv} in comparison with all the other polymers, indicating greater polymer wettability. Furthermore, the (θ_{adv}) increased with increasing the molar mass of the alcohol applied in the polymer synthesis. This was expected, as ethylene glycol is the most hydrophilic monomer and increasing the aliphatic chain fraction could contribute to a decrease on the water adhesion on the polymer surface (Tab. 3).

Tab. 3. Biofilm formation on, and water advancing (θ_{adv}) and receding (θ_{rec}) contact angles of the polymer films.

	C. tropicalis[1]		*C. albicans*[1]		Contact angle [°]	
Sample	**72A**	**72P**	**DEB14**	**Ca04**	θ_{adv}	θ_{rec}
PVC	5.35	4.69	4.79	4.79	n.a.[2]	n.a.[2]
PCL	0	4.39	0	0	73.7 ± 2.5	55.2 ± 2.4
PES	0	0	0	0	60.3 ± 0.3	33.2 ± 1.9
PPS	5.32	4.57	n.a.[2]	n.a.[2]	64.7 ± 3.0	35.2 ± 0.3
PBS	0	5.00	n.a.[2]	n.a.[2]	68.5 ± 1.1	42.2 ± 0.9

[1] Colony formation unities (**log CFU/cm²**); [2] not applied

In general, the receding contact angle (θ_{rec}), which is measured in the immersion phase of the sample from water, is influenced more than the advanced contact angle by the strength of interactions between water and hydrophilic domains of the polymer surface.[19] The antifouling ability of polymers has been related to the formation of a tightly bound water layer, on the polymer surface, that hinders the surface adsorption of fungi and bacteria. Low θ_{rec} can be considered suitable parameter for predicting the anti-adhesive properties of materials. The θ_{rec} showed similar behavior with closer values among the synthesized polyesters (Tab. 2), showing much lower values when compared with PCL and pointing out a greater wettability of PES, PPS and PBS polyesters. The PES was able to completely prevent the *C. tropicalis* and *C. albicans* biofilm formation, which seems to be partially related to its low θ_{adv} and θ_{rec}. Interestingly, also in addition to being a good antibiofilm material, PCL presented the highest θ_{adv} and θ_{rec} values. This result suggests that the antibiofilm activity of the polymers was not exclusively affected by fungal cell adhesion on the polymer surface, but also by the influence of polymer chemical composition and properties, *e.g.* H-bonding capacity, on fungal cell toxicity.[34]

It is important to highlight that *Candida albicans* is reported to form biofilm on several different biomedical devices, made of a variety of materials; such as PVC, polymethyl-methacrylate, silicon, polyurethane, polycarbonate, and polypropylene.[35,36] Among previous studies, a trend for the extent of biofilm formation could be observed, where; polystyrene > polycarbonate > PVC > silicone.[37] Various properties including roughness of the substrates and surface free energy may influence adhesion and biofilm development, but recent reports have shown that they have a secondary role on *C. albicans* biofilm formation when compared to characteristic properties of the strains.[38] These properties may include cell-surface hydrophobicity, growth rate, adhesion formation and, as a consequence, they depend on the substrate material chemical composition.[39] Therefore, *C. albicans* cell surface hydrophobicity is long known to be a putative virulence factor,[40] and the cells having more hydrophobic nature usually show maximum capability of biofilm formation and biodegradation. Thus, although different clinical isolates exhibited different cell wall physico-chemical properties, biofilm adhesion to hydrophobic substrata occurs to a greater extent than to hydrophilic surfaces.[41]

Hemolytic activity and cell viability

Before implanting polymer-based medical devices into the human body, their evaluation on mammalian cell toxicity assays is of utmost importance. Consequently, the polymers which presented the best antibiofilm performances (PES, PBS and PCL) were analyzed for their toxicological effects on human blood cell lysis. The hemolytic activity of the polymers was tested in comparison with the broadly used systemic antifungal agent AmB, in which hemolysis is a common side effect of its therapeutic application (Fig. 4).[42,43] For PES, no significant human blood cells lysis (< 5.2 % of hemolysis) could be detected at the maximum polymer concentration evaluated (10 µg of PES, corresponding to 1.4 g of polymer in human blood). In comparison, applying the same concentrations and incubation times (24 h), AmB presented ~ 96 % of hemolysis and PCL (control polymer) ~ 11 % of hemolysis. PBS showed similar hemolysis (~ 10 %) as PCL at the same concentrations.

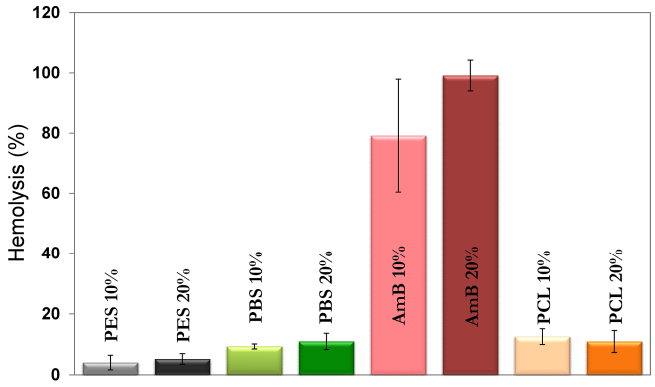

Fig. 4 Percent hemolysis caused by the polymers at different concentrations (polymer wt% per blood volume) after 24 h incubation at 37 °C.

Other polymers with antibiofilm properties against drug-resistant *Candida* isolates presented similar hemolytic activity,[19] where less than 9% (after 1 h incubation) of hemolytic activity was found, as well as, values ~ 3 % for polymer micelles (after 3 h incubation).[44] According to the aforementioned values, we can infer that PES and PBS demonstrate excellent non-hemolytic activity, being potentially safe to be implanted into the human body.

By using a human fibroblast (HF) cell culture model, the cell viability on the synthesized polymer surfaces was evaluated. The cytotoxicity to HF, caused by the three synthesized biopolymers (PES, PPS and PBS) was tested also using as reference the well-known FDA-approved and environmentally friendly PCL. In Fig. 5 it is demonstrated that all three succinic based polyesters (PES, PPS and PBS) present negligible toxicity at concentrations up to 1000 $\mu g \cdot mL^{-1}$.

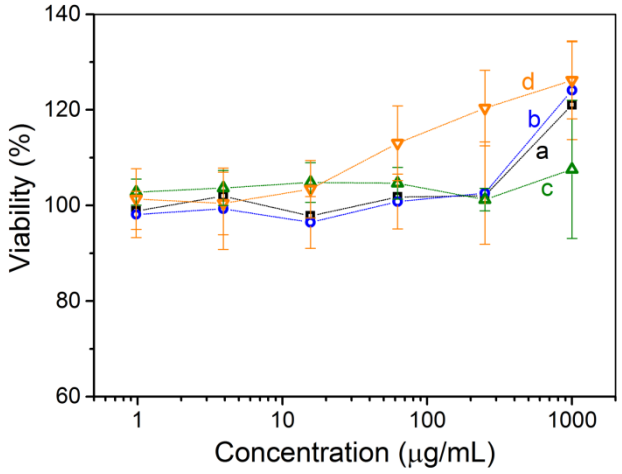

Fig. 5 Human fibroblast (HF) cell viability experiments in the presence of (a) PES, (b) PPS, (c) PBS and (d) PCL (reference), after 48 h of incubation.

The results demonstrated that none of the tested polymers affect significantly the cell viability. The absence of cytotoxicity was expected, as the degradation products, *e.g.* succinic acid, are intermediates in the tricarboxylic acid cycle (citric acid cycle), and the alcohols employed for the polymer preparation are inert (ethylene glycol, propylene glycol and butanediol).[45,46]

Human stem cells proliferation

In vitro proliferation tests of cells growing on the test material often serve as an important initial test of biocompatiblity.[47] Thus, also the behaviour of human mesenchymal stem cells (hMSC), largely used in tissue engineering,[48,49] was evaluated as cell line model for *in vitro* polymer biocompatibility testing. The cellular attachment is the first step in evaluating the hMSC biocompatibility with a polymer, as significant structural cell changes can occur.

The polymer's effect on hMSC cell morphology, after 1 day cell culture, is shown in Fig. 7. The reference synthetic polymer PCL induced an irregular morphology to the cells, where they seem to grow more randomly (or freely) over the polymer surface (Fig. 7d). Differently, the succinate-based biopolymers show a correlation between their chemical structure and the hMSC morphology. The PBS (presenting butyl aliphatic segments) induce the stem cells to grow with a wider structure (Fig. 7c), representative of osteoblast cells.[47] On the other hand, the PPS (presenting shorter propyl segments) induce the cells to a thinner structure (Fig. 7b). This is even more defined for PES (with ethyl segments), which induces the cells to form very thin and elongated structures, characteristic of fibroblast cells.

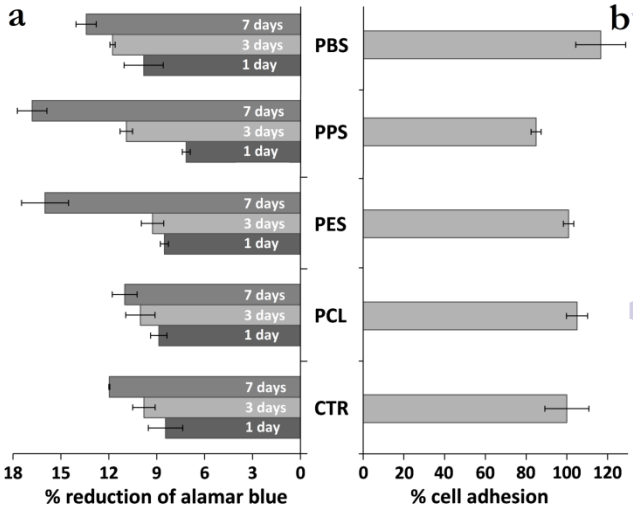

Fig. 6 hMSC proliferation assay on the materials after 1, 3 and 7 days of cell culture (a) and cell adhesion assay after 24 h of cell culture (b) (alamarBlue® assay).

Furthermore, the quantitative cell proliferation after 1, 3 and 7 days (Fig. 6a) and cell attachment results after 24 h demonstrate that the morphology changes could be dependent on the polymers' induction to cell growth and adhesion. The highest cell adhesion value was obtained for PBS, achieving about 120% cell attachment and the lowest result was obtained for PPS with an ~80% adhesion (Fig. 6b). However, evaluating the cell proliferation on a longer term (after 3 and 7 days, Fig. 6a), it is possible to observe how the cells develop after adapting to the systems. After the 7th day all three polyesters present higher cell proliferation than PCL and the control, where PES and PPS seem to be the best among all materials. This indicates that the formation of a narrower cell morphology requires an induction period, where the cells get acquainted to the new, more ordered

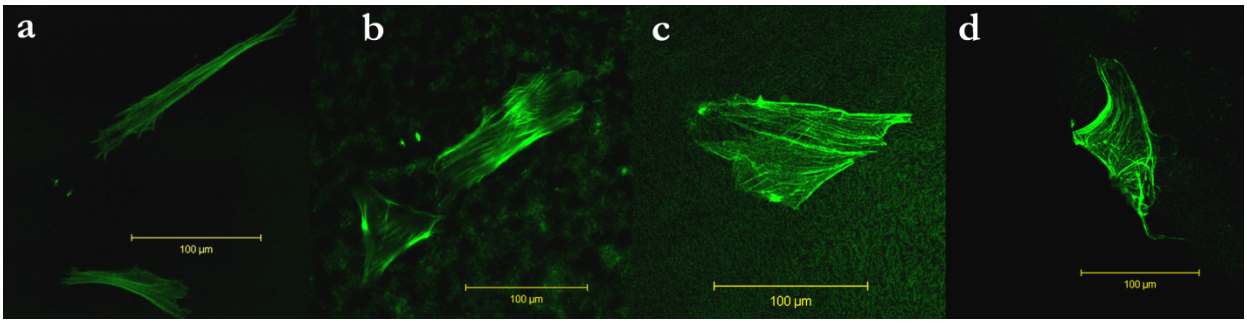

Fig. 7 Confocal images of hMSC morphology and cell-material interaction on PES (a), PPS (b), PBS (c) and reference PCL (d) polyesters after 24 h culturing.

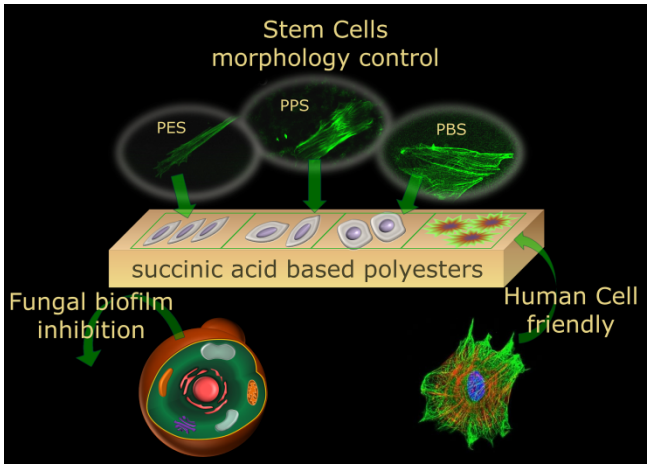

Scheme 1 Succinic acid based polyesters schematic summary of properties.

environment. The results demonstrate that the succinate based polyesters are not only nontoxic but exert a positive influence on hMSC proliferation. This representative proliferation differences and morphology changes are not only a sign of good cell compatibility and affinity to the polymers, but also of cell morphology control based on the polymer chemical structure.

Taking into account that the hydrophilicity decreases from PES to PBS and the reference PCL is the most hydrophobic (Tab. 3), the biopolymer hydrophilicity seems to take part into the differences observed on the cell proliferation (Fig. 6). Studies have shown that chemical functionality and hydrophilicity have important roles in cell adhesion and function. Some research groups[50,51] reported that the carboxylic acid groups onto polymer surfaces, even though they were negatively charged, show better cell attachment and proliferation than their counterpart hydrophobic surfaces. It is important to mention that each synthetized biopolymer presented herein are carboxyl or hydroxyl terminated, due to the synthetic path applied (polycondensation polymerisation, *vide* infra).

In summary, the materials structure and surface have shown to have different effects on fungal and mammalian cells. The materials which promoted positive effects on the cell proliferation were also unfavourable for fungal cell growth (Scheme 1). This cell selectivity gives to these materials a great potential of exploration as materials for medical application. Thus, the aforementioned biopolymers can fulfil the task of selectively stimulating the hMSC cells growth and proliferation while preventing its potential inhibitors (*e.g.*, fungi contamination).

Conclusions

The properties of biodegradable and biocompatible biopolymers PES, PPS and PBS with emphasis on their new possible applications are reported herein. The polymers were successfully synthesized, fully characterized and evaluated as for their mechanical and thermal properties. PPS was the softest biopolymer showing low energy to break, tensile strength and elongation at break. In contrast, the PES and PBS showed high Young modulus, tensile strength and energy to break; outperforming the commercial (PVC) catheter. Furthermore, the biopolymers demonstrated intrinsic action against the strong biofilm formers *C. albicans* and *C. tropicalis*, opening an opportunity to substantially reduce the incidence of device associated infections in invasive medical devices. While PBS demonstrated efficient antifungal activity only against drug-resistant clinical isolates of *C. tropicalis*, PES presented a broader action, efficiently preventing biofilm growth of all *C. albicans* and *C. tropicalis* strains. Moreover, they also have shown excellent *in vitro* biocompatibility with mammalian cells, as well as non-hemolytic activity in human blood. When hMSC cells were in contact with the biopolymers, morphological changes were observed as cell proliferation *in vitro* was influenced by the polymer structural characteristics. These findings suggest that hydrophilicity and negative charge characteristics, as well as polymer wettability (PES) play important roles on the growth and proliferation of hMSCs. It is important to highlight that the fungal inhibition is due to the intrinsic characteristics of the polymer material itself, which the efficacy could be further enhanced by the incorporation of a second agent; such as antibiotics, antiseptics or antimicrobial compounds.

Experimental

Materials

Ethylene glycol (EG, Sigma-Aldrich), 1,3-propanediol (PD, Sigma-Aldrich), 1,4-butanediol (BD, BASF), succinic acid (SA, Aldrich Chemie), acetone (ACT) (CZ, Merck), Tetrahydrofuran (THF) (CZ, Merck), Dimethylformamide (DMF) and Acetonitrile (ACN) were used as received. Titanium tetraisopropoxide (TTiPO), Amphotericin B trihydrate (AmB), and poly-ε-caprolactone (PCL – 10kDa) were purchased from Sigma-Aldrich. A commercial Polyvinylchloride (PVC) catheter (Mark Med, number 12) was used as reference. The water used was pre-treated with the Milli-Q® Plus System (Millipore Corporation).

Polyester synthesis

The polymers were synthesized following a previously described two-step melt polycondensation (esterification and polycondensation) protocol.[52] Briefly, in a glass reactor were loaded SA, the proper amount of glycols in molar ratio 1/1.2 and the catalyst TBT (4 x 10^{-4} mol/mol diacids). The vessel was further evacuated and filled with argon. The reaction mixture was heated at 200 °C and stirred at constant speed (500 rpm). This first step (esterification) was considered complete when the theoretical H_2O yield was removed from the reaction mixture by distillation and collected in a graduate cylinder. The polycondensation reaction was carried out at 250 °C, ~ 0.03 atm, under stirring at a constant speed (700 rpm) and it has been completed after 4 h. The copolyester was purified *via* dissolution in chloroform and precipitation with methanol.

Characterisation techniques

Nuclear magnectic resonance analysis (*NMR*): ^{1}H NMR and ^{13}C NMR spectra (300 and 75 MHz, respectively) were obtained using a Bruker Avance DPX 300 NMR spectrometer with $CDCl_3$ as the solvent at 25 °C. The chemical shifts are relative to TMS using hexamethyldisiloxane (HMDSO, 0.05 and 2.0 ppm from TMS in ^{1}H NMR and ^{13}C NMR spectra) as internal standard. Typical conditions were as follows: π/2 pulse width 15.6 μs, relaxation delay 10 s, spectral width 6 kHz, aquisition time 4.95 s, 32 scans for ^{1}H NMR, and π/2 pulse width 9.9 μs, relaxation delay 10 s, spectral width 20 kHz, aquisition time 1.61 s, 5000-10000 scans for ^{13}C NMR.

Size exclusion chromatography (SEC): The number average molecular weight (M_n) and molecular weight distribution (polydispersity, M_w/M_n) of the synthesized copolymers were determined by SEC. Tetrahydrofuran (THF) was used as the mobile phase at a flow rate 0.5 mL·min^{-1}. The injection-loop volume was 0.1 mL. Measurements were performed with triple viscosity/concentration/light scattering detection. The set was connected to a DAWN DSP-F light-scattering photometer (Wyatt Technology Corp.), a Viscotek model TDA 301 modified differential viscometer (without internal light scattering and concentration detectors) and a Shodex RI 71 differential refractometer. The data were accumulated and processed using the Astra and triSEC software packages.

Thermal analysis: The differential scanning calorimetry (DSC) measurements were performed with a Perkin-Elmer Pyris 1 DSC calorimeter. Samples of about 5 mg were closed in aluminum sample pans, and the system was flushed with dry helium during the DSC scan. The temperature scale was calibrated according to the melting points of cyclohexane and indium. The power output scale was calibrated with indium. The samples were scanned in the 0 – 160 °C temperature interval in the standard DSC mode with constant heating rate 10 °C/min in heating and cooling runs. The DSC curves were evaluated by standard Perkin Elmer software.

The thermal gravimetric analyses (TGA) were performed on a TA Instruments Q50 thermogravimetric analyzer. The TGA instrument was calibrated using nickel. An average sample weight of 8-12 mg was placed in a platinum pan and heated at 10 °C/min from 30 to 900 °C under a nitrogen flow.

Mechanical analysis: The samples were prepared in open molds by melting at 120 °C and further bubbles evaporation in a vacuum oven (120 °C; 30 min). Obtained films were conditioned one day in an desiccator - before mechanical testing.

Dynamic mechanical and thermal analysis (DMTA): The samples were measured using ARES G2 rheometer (TA Instruments). The samples were measured by oscillatory shear deformation at a constant frequency of 1Hz and the rate of heating 3 °C/min. The dependence between storage (*G*') and loss shear modulus (*G*'') in the range of -100 - 100 °C was determined. Specimens with the following dimensions were used: length = 20 mm, width = 10 mm and thickness = 1 mm.

Tensile tests: Tensile tests were carried out on Instron 6025 instrument (High Wycombe, UK) at room temperature and at test speed of 1 mm/min. The samples were prepared in an open mold by melting at 120˚C and further drying in a vacuum oven (120˚C; 30 min) for preventing bubbles formation. The obtained films were conditioned for one day in a desiccator. At least nine dumb-bell shaped specimens (35 mm × 2 mm × (1 ± 0.1 mm)) were tested from each system and the final value was an average from at least five measurements. The Young modulus, tensile strength, elongation at break and energy to break were evaluated.

Polymer particles preparation: Nanoparticles (NPs) were prepared from the 3 different polyesters and the control polymer (PCL) by using the nanoprecipitation protocol. The polyesters were first completely dissolved in acetone at 40 °C and subsequently the solution was added drop-wise (EW-74900-00, Cole-Parmer®) to pure water (Milli Q®) (20 mL) under stirring (500 rpm). The organic solvent was further removed by evaporation under vacuum at room temperature and the aqueous solution was concentrated to 5 mL. The prepared NPs were used immediately (hemolysis assays, cell culture and *in vitro* cell viability experiments, *vide infra*) or stored at 4 °C.

Antifungal assay

Fungal isolates: Two Fluconazole, Amphotericin B (AmB), Voriconazole and Anidulafungin resistant clinical isolates of *C. tropicalis* (72A and 72P), a *C. albicans* clinical isolate (DEB14) and a commercial strain of *C. albicans* (Ca04) were used in this study. The fungal strains are deposited in the Mycology Collection of the Universidade Federal do Rio Grande do Sul-UFRGS, Porto Alegre, Brazil.

Biofilm formation assay on polymers and tracheal catheter material: The applied methodology is an adaptation from the literature.[12] Initially, the yeasts were grown in Sabouraud Agar for 24 h at 37 °C to obtain pure young colonies. Seven colonies were added to 2 mL of Tryptose Soy Broth (TSB) and incubated for 24 h at 37 °C. Discs of 1 cm were cut from the PVC catheter and the polyesters. These were added to 9 mL of peptone water containing 1 ml of the inoculum of TSB colonies and incubated for 96 h at 37 °C. The strong biofilm producer yeasts, as characterized previously,[12] were used to determine their biofilm formation capacities. Subsequent to the incubation period, the discs were washed three times with peptone water for removal of poorly adhered cells. The catheter discs were added to another flask with 50 mL of peptone water and the adhered cells were released from the catheter by sonication at a frequency of 40 kHz for 10 min. The dilution of the sonicated water phase by a factor of 10 allowed the determination of the colony formation unities (CFU), and 20 µL of each dilution was seeded in Sabouraud Agar. The plates were incubated for 24 h at 37 °C and the $CFU.cm^{-2}$ values were determined. For an easier comparison among the different strain results, the $CFU.cm^{-2}$ values are presented in logarithmic scale. All counts were made in duplicate and each experiment was repeated twice.

Determination of polymer surface wettability by contact angle measurements

Substrate preparation: Microscopic glass slides were cut into 2.6×3.8 cm pieces, sonicated in methanol and deionized in water for 30 min and heated at 130 °C for 2 h. Dry samples were exposed to air plasma (25 W, Harrick Plasma Cleaner) for 5 min just before polymer deposition.

Polymer Coatings: PCL, PES, PPS and PBS thin films were spin-coated on treated glass substrates from 5 $mg{\cdot}mL^{-1}$ solutions in chloroform using PWM32-PS-R790 spinner (Headway Research, Inc.). 500 µL of polymer solution was applied on each glass substrate and spin-coated at 1000 rpm for 60 s. Polymer films were annealed at 70 °C for 1 h under vacuum.

Contact angle: The wettability of surfaces was examined by dynamic sessile water drop method using a DataPhysics OCA 20 contact angle system. A 5 µL drop was placed on the surface, and advancing (θ_{adv}) and receding (θ_{rec}) contact angles were determined while the volume of the drop was increased up to 10 µL and decreased at flow rate of 0.5 $\mu L{\cdot}min^{-1}$. Data were processed by Laplace-Young fitting algorithm. Reported values are averages of at least three measurements recorded at different positions on each substrate.

Hemolysis assays

Hemolysis experiments were performed to verify the *in vitro* blood compatibility of the polymers and controls for future application as polymer-based medical devices following previous published methodology.[33] Whole blood was collected from healthy human volunteers in an evacuated siliconized glass tube containing EDTA as anticoagulant. Briefly, 2.5 µL (5 µg of polymer) and 5.0 µL (10 µg of polymer) of each polymer were placed in centrifuge tubes, followed by the addition of 50 µL of human blood and incubated at 37 °C for 2 h. After this period of time, 6.5 mL of 0.9% NaCl aqueous solution was added to stop the hemolysis process and the samples were incubated at 37 °C for further 1 h. The positive control was prepared by adding 50 µL of blood to 6.5 mL of distilled water. The negative control was obtained by adding 50 µL of 0.9% NaCl aqueous solution to 6.5 mL of ultrapure water. After incubation, the samples were centrifuged for 30 minutes at 4400 rpm. The absorbance of the hemoglobin was detected at 540 nm (UV-Vis 1601 PC Spectrophotometer, Schimadzu, Japan). The percentage of hemolysis was calculated using the following equation:

$$\%Hemolysis = \frac{ABS(sample) - ABS(-control)}{ABS(+control) - ABS(-control)} x100$$

where ABS represents absorbance. The absorbance values of the positive and negative controls were 0.9600 and 0.00[illegible], respectively.

Cell culture and *in vitro* cell viability experiments

In vitro cell culture: Human Mesenchymal Stem Cells (hMSC) were obtained from LONZA (Milano, Italy). hMSC were cultured in 75 cm^2 cell culture flask in Eagle's alpha Minimum Essential Medium (α-MEM) supplemented with 10% Fetal Bovine Serum (FBS), antibiotic solution (streptomycin 100 $\mu g{\cdot}mL^{-1}$ and penicillin $100U{\cdot}mL^{-1}$, Sigma Chem. Co) and 2 mM L-glutamine. The human fibroblast (HF) cells were cultivated in Dulbecco's Modified Eagle's Medium (DMEM) supplemented with 10% FBS, penicillin $100U{\cdot}mL^{-1}$ and streptomycin 100 $\mu g{\cdot}mL^{-1}$ (Life Technology, CZ). hMSCs at 4th passage were used for the experimental procedures. All cells were incubated at 37°C in a humidified atmosphere with 5% CO_2 and 95% air.

Viability test: To evaluate cell biocompatibility on biopolymer surfaces, hMSC were plated at concentration of 5.000 $cells{\cdot}well^{-1}$ in triplicate onto different biopolymers. The medium in cell-load gel materials culture plates were removed after cultured for 1, 3 and 7 days and the *in vitro* cell viability was checked by the alamarBlue® assay (AbDSerotec, Milano, Italy). This assay quantified the redox indicator which changed to a fluorescent product in response to the chemical reduction by mitochondrial enzymes such as flavin mononucleotide dehydrogenase, flavin adenine dinucleotide dehydrogenase and nicotinamide adenine dinucleotide dehydrogenase. In addition, a redox phenomenon gave a quantitative indication of metabolic activity of live cells. An aliquot of 500 µL of alamarBlue® diluted 1:10 in phenol red-free medium was added to each well and incubated for a further 4 h at 37°C, 5% CO[illegible]. Later, 100µL of this solution was transferred into a 96 well plate for colorimetric analysis. Wells without any cells were used to correct any background interference from the redox indicator. The optical density was immediately measured with a spectrophotometer (Sunrise, TECAN, Männedorf, Zurich, Switzerland) at wavelengths of 540 and 600 nm. The cell viability percentage was evaluated according to th[illegible]

manufacturer's protocol. The culture medium during experimental time was changed every two days.

To evaluate the toxicity of biopolymer nanoparticles on HF fibroblasts, the cells were seeded at a density of 5.000 cells·well^{-1} in triplicates in 96 well plates. For particle addition on the following day, the volume was calibrated to 80 µL, and 20 µL of the 5-times concentrated dilution of particle dispersion were added per well to a final polymer concentration ranging from 1 to 1000 µg·mL^{-1}. After incubation of the cells with the polymer for 48 h, alamarBlue® reagent was added and incubated a minimum for 3 h at 37 °C before the fluorescence signal was read out. All cells experiments are average of at least 3 measurements. The fluorescence intensity of the untreated control samples was set as '100% cell viability,. The fluorescence signal of '0% viability samples, (were all cells were killed by addition of hydrogen peroxide) was subtracted as background.

Cell adhesion and morphology: For cell adhesion tests, hMSC were plated at concentration of 5000 cells·well^{-1} in triplicate onto biopolymer films. The cell adhesion values after 24 h were presented as the cellular percentage of attached cells in relation to control tissue plates (CTR). They were obtained from alamarBlue® consumption (absorbance measured at 540 and 600 nm), considering that the control cells (CTR) have adhered 100%. The cell morphology and cell spreading pattern interaction of hMSC onto the biopolymers were evaluated by confocal laser scanning microscopy (LSM 510, CarlZeiss). Briefly, hMSCs at 5000 were seeded onto the materials and incubated for 24 h. At the end of the incubation time, the non-attached cells were removed by rinsing carefully three times with a phosphate buffer solution and then incubated with CellTracker™ GreenCMFDA in phenol red-free medium at 37 °C for 30 min. Subsequently cell culture was washed with phosphate buffer solution and incubated for 1 h in complete medium. After this period of time the cells were visualized on LSM.

Acknowledgements

The research leading to these results has received funding from the Norwegian Financial Mechanism 2009-2014 and the Ministry of Education, Youth and Sports under Project Contract no. MSMT-28477/2014. The Ministry of Industry and Trade of the Czech Republic (grant # MPO TIP FR-TI4/625) is also acknowledged. Authors are thankful for the Science without Borders CNPq Special Visiting Scientist Fellowship of Luigi Ambrosio. R.K. Donato is thankful to FAPERGS/CAPES for the DOCFIX postdoctoral fellowship. C.G.Venturini acknowledges the Program Science without Borders CAPES/Brasil (Process number 2293/13-7).

Notes and references

1 J.C. Middleton and A.J. Tipton, *Biomaterials* 2000, **21**, 2335.
2 C.K. Pillai and C.P. Sharma, *J. Biomater. Appl*., 2010, **25**, 291.
3 C. von Eiff, B. Jansen, W. Kohnen and K. Becker, *Drugs* 2005, **65**, 179.
4 E.M. Kojic and R.O. Darouiche, *Clin. Microbiol. Rev*., 2004, 17, 255.
5 B. H. Bowman, J. W. Taylor and T.J. White. *Mol. Biol. Evol*., 1992, **9**, 893.
6 G.D. Brown, D.W. Denning, N.A. Gow, S.M. Levitz, M.G. Netea, T.C. White, *Sci. Transl. Med*., 2012, **4**, 165rv13.
7 J.A. Sangeorzan, S.F. Bradley, X. He, L.T. Zarins, G.L. Ridenour, R.N. Tiballi, C.A. Kauffman, *Am. J. Med*. 1994, **97**, 339.
8 G.P. Bodey, M. Mardami, H.A. Hanna, M. Boktour, J. Abbas, E. Girgawy, R.Y. Hachem, D.P. Kontoyiannis, I.I. Raad, *Am. J. Med*. 2002, **112**, 380.
9 D.L. Horn, D. Neofytos, E.J. Anaissie, J.A. Fishman, W.J. Steinbach, A.J. Olyaei, K.A. Marr, M.A.Pfaller, C-H- Chang, K.M. Webster, *Clin. Infect. Dis*., 2009, **48**, 1695.
10 R.M. Donlan, Emerg, *Infect. Dis*., 2001, **7**, 277.
11 G. Ramage, J.P. Martinez, J.L. Lopez-Ribot, *FEMS Yeast Research* 2006, **6**, 979.
12 V.Z. Bergamo, R.K. Donato, D.F. Dalla Lana, K.Z. Donato, G.G. Ortega, H. S. Schrekker, A.M. Fuentefria, *Lett. Appl. Microbiol*., 2014, **60**, 66.
13 P. Uppuluri, A. Srinivasan, A. Ramasubramanian, J.L. Lopez-Ribot, *Antimicrob. Agents Chemother*., 2011, **55**, 3591.
14 L.Y. Chai, D.W. Denning, and P. Warn, *Crit. Rev. Microbiol*., 2010, **4**, 282.
15 S.P. Hawser and L.J. Douglas, *Antimicrob. Agents Chemother*., 1995, **39**, 2128.
16 M. Nucci and A.L. Colombo, *Diagn. Microbiol. Infect. Dis*., 2007, **58**, 77.
17 H.S. Schrekker, R.K. Donato, A.M. Fuentefria, V. Bergamo, L.F. Oliveira, M.M. Machado, *MedChemComm* 2013, 1457.
18 S. Silva, M. Negri, M. Henriques, R. Oliveira, D.W. Williams, J. Azeredo, *FEMS Microbiol. Rev*. 2012, **36**, 288.
19 I. Francolini, G. Donelli, C. Vuotto, F.A. Baroncini, P. Stoodley, V. Taresco, A. Martinelli, L. D'Ilario, A. Piozzi, *Pathog. Dis*., 2014, **70**, 401.
20 D. Campoccia, L. Montanaro and C.R. Arciola, *Biomaterials* 2013, **34**, 8553.
21 R. Liu, X. Chen, S.P. Falk, K. S. Masters, B. Weisblum, S.H. Gellman, *J. Am. Chem. Soc*., 2015, **137**, 2183.
22 C.S. Ha and J.A. Jr. Gardella, *Chem. Rev*., 2005, **105**, 4205.
23 M.G. Raucci, V.D' Antò, V. Guarino, S. Martina, R. Valleta, L. Ambrosio, *J. Tissue Eng. Regen. Med*., 2013, DOI:10.1002/term.1768.
24 M.G. Raucci, M.A. Alvarez-Perez, C. Demitri, D. Giugliano, V. De Benedictis, A. Sannino, L. Ambrosio, *J. Biomed. Mater. Res. A*., 2015, **103**, 2045.
25 F. Cobo, J.L. Cortés, C. Cabrera, A. Nieto, A. Concha, *Cell Biol. Int*., 2007, **31**, 991.
26 D.N. Bikiaris, G.Z. Papageorgiou, and D.S. Achilias, *Polym. Degrad. Stabil*., 2006, **91**, 31.
27 G.Z. Papageorgiou and D.N. Bikiaris, *Polymer* 2005, **46**, 12081.
28 S. Pannanusorn, V. Fernandez, and U. Romling, *Mycoses* 2013 **56**, 264.
29 A.A. Popoola, I. Oseni, K.T. Bamgbola, A.L. Babata. *Afr. J. Urol*., 2012, **18**, 157.
30 J.C.O. Sardi, L. Scorzoni, T. Bernardi, A.M. Fusco-Almeida, M.J.S. Giannini, *J. Med. Microbiol*., 2013, **62**, 10.
31 T.-F.C. Mah and G.A. O'Toole, *Trends Microbiol*., 2001, 34.
32 K. Grundke, K. Pöschel, A. Synytska, R. Frenzel, A. Dreschler, M. Nitschke, A.L. Cordeiro, P. Uhlmann, P.B. Welzel. *Adv. Colloid Interface Sci*., 2015, **222**, 350.
33 C. Sipahi, N. Anil and E. Bayramli, *J. Dent*., 2001, ***29***, 197.
34 S. Chen, L. Li, C. Zhao, J. Zheng, *Polymer* 2010, **51**, 5283.
35 E.M. Kojic, R.O. Darouiche, *Clin. Microbiol. Rev*., 2004, 17, 255.

36 G. Ramage, J.P. Martinez and J.L. Lopez-Ribot, *FEMS Yeast Res*., 2006, **6**, 979.
37 J. Raut, V. Rathod, S.M. Karuppayil, *Jpn. J. Med. Mycol*., 2010, **51**, 131.
38 W.J. da Silva, J. Seneviratne, L.P. Samarnayake, A.A. Del Bel Cury, *J. Biomed. Mater. Res. B. Appl. Biomater*., 2010, **94**, 149.
39 R.B. Shinde, J.S. Raut and M.S. Karuppayil, *Mycoscience* 2012, **53**, 220.
40 W.B. Hazen and K.C. Hazen, *FEMS Microbiol. Lett*., 1989, **57**, 167.
41 N. Cerca, G.B. Pier, M. Vilanova, R. Oliveira, J. Azeredo, *Res. Microbiol*., 2005, **156**, 506.
42 P. Legrand, E.A. Romero, B.E. Cohen, J. Bolard, *Antimicrob. Agents Chemother*., 1992, **36**, 2518.
43 M.L. Adams and G.S. Kwon, *J. Control. Release* 2003, **87**, 23.
44 X. Yang, D. Cao, N. Wang, L. Sun, L. Li, S. Nie, Q. Wu, X. Liu, C. Yi, G. Gong, *J. Pharm. Sci*., 2014, **103**, 305.
45 H. Li, J. Chang, A. Cao, J. Wang, *Macromol*., *Biosci*., 2005, **5**, 433-440.
46 H. Wang, M. Xu, Z. Wu, W. Zhang, J. Ji, P.K. Chu, *ACS Appl. Mater. Interfaces* 2012, **4**, 4380-4386.
47 C.J. Kirkpatrick, F. Bittinger, M. Wagner, H. Kohler, T.G. Vankooten, C.L. Klein, M. Otto, *P. I. Mech. Eng. H*., 1998, **212.2**, 75.
48 M.G. Raucci, M.A. Alvarez-Perez, S. Meikle, L. Ambrosio, M. Santim, *Tissue Eng. Part A*., 2014, **20**, 474.
49 J. M. Anderson, M. Kushwaha, A. Tambralli, S. L. Bellis, R. P. Camata, H.-W. Jun, *Biomacromolecules* 2009, **10**, 2935.
50 D. Bhattacharyya, H. Xu, R.R. Deshmukh, R.B. Timmons, K.T. Nguyen, *J. Biomed. Mater. Res. A*., 2010, **94**, 640.
51 C.-H. Jou, J.-S. Lee, W.-L. Chou, D.-G. Yu, M.-C. Yang, *Polym. Adv. Technol*., 2005, **16**, 821.
52 E. Jäger, A. Jäger, P. Chytil, T. Etrych, F. C. Giacomelli, B. Říhová, P. Štěpánek and K. Ulbrich. J. Control Release, 2013, 165, 153.